

CARBON MICROFIBER MATERIAL FOR ELECTROMAGNETIC  
(SHIELDING) APPLICATIONS

A Dissertation  
Submitted to the Graduate Faculty  
of the  
North Dakota State University  
of Agriculture and Applied Science

By

Muhammad Nadeem Rafiq

In Partial Fulfillment of the Requirements  
for the Degree of  
DOCTOR OF PHILOSOPHY

Major Department:  
Electrical and Computer Engineering

September 2015

Fargo, North Dakota

# NORTH DAKOTA STATE UNIVERSITY

Graduate School

---

## Title

Carbon Microfiber Material for Electromagnetic (Shielding) Applications

---

## By

Muhammad Nadeem Rafiq

---

The supervisory committee certifies that this *disquisition* complies with North Dakota State University's regulations and meets the accepted standards for the degree of

## DOCTOR OF PHILOSOPHY

### SUPERVISORY COMMITTEE:

Dr. Benjamin D. Braaten

---

Chair

Dr. David A. Rogers

---

Dr. Dr. Ivan T. Lima Jr.

---

Dr. Yechun Wang

---

Approved:

Sep 11, 2015

---

Date

Scott C. Smith

---

Department Chair

## ABSTRACT

Electromagnetic shielding is becoming more and more important with the abundance of wireless devices. Therefore a need has arisen for more versatile, flexible and low-cost solutions for shielding. For these requirements, carbon microfiber material has been proposed for electromagnetic shielding applications. For this purpose its shielding effectiveness has been measured and modeled in a simulation environment. A parametric simulation was conducted for the material property 'conductivity' and the results were compared to measured ones. These simulation results were also verified by the analytical solution for the shielding effectiveness and the agreement between the simulated values and analytical results demonstrated that the carbon microfiber material, though having less conductivity than the traditional metallic shields is a good candidate for electromagnetic shielding applications. Carbon microfiber not only provides comparable shielding effectiveness to a metallic shield but it can be advantageous because of its light weight, corrosion resistance and flexibility. Also, its porous nature can help with cooling of enclosed electronic circuits.

## ACKNOWLEDGMENTS

I am sincerely grateful to my advisor Dr. Benjamin D. Braaten for his support throughout my PhD program. I cannot thank him enough for his patience and motivation. He is a thorough gentleman who leads the way. Not only did he inculcate the academic knowledge but also presented the moral and ethical examples to follow.

Also I would like to express my appreciation to my committee members, Dr. David A. Rogers, Dr. Ivan T. Lima Jr. and Dr. Yechun Wang for their support and time during my research work.

I also thank my fellow PhD candidate and labmate Mr. Adnan Iftikhar for his support which was always present for me.

Lastly, I would thank my family, my parents, my wife and my beautiful children for their continuous support and understanding. They all are part of this whole effort.

# DEDICATION

To my wonderful family

# TABLE OF CONTENTS

ABSTRACT .....	iii
ACKNOWLEDGMENTS.....	iv
DEDICATION.....	v
LIST OF FIGURES.....	viii
LIST OF SYMBOLS .....	x
CHAPTER 1. INTRODUCTION & LITERATURE REVIEW .....	1
1.1. Introduction .....	1
1.2. Literature Review .....	4
1.2.1. Carbon nanotubes / nano-fibers .....	4
1.2.2. Flexible graphite and colloidal graphite for shielding.....	6
1.3. Conclusions .....	7
CHAPTER 2. THEORY OF ELECTROMAGNETIC SHIELDING .....	9
2.1. Wave Impedance.....	10
2.2. Shielding Effectiveness .....	11
2.3. Reflection Loss.....	12
2.4. Absorption Loss.....	14
2.5. Correction Factor / Multiple Reflections in Thin Shield.....	15
CHAPTER 3. MEASUREMENTS .....	17
CHAPTER 4. SIMULATION OF CARBON MICROFIBER SHIELD .....	25
4.1. Simulation Setup .....	25
4.2. Measurement Results .....	27

CHAPTER 5. ANALYTICAL FORMULATION AND COMPARISON OF RESULTS .....	31
5.1. Comparison of Results .....	33
5.2. Conclusions .....	35
BIBLIOGRAPHY .....	37

## LIST OF FIGURES

<u>Figure</u>	<u>Page</u>
1. Carbon microfiber sample for shielding .....	2
2. Single wall carbon nanotube and multiwall carbon nanotube [23].....	4
3. Liquid crystal polymer [24].....	5
4. Graphite material [25] (a) Single carbon atom (b) Flexible graphene material .....	7
5. Shielding application for shielded source and receptor.....	9
6. Partial reflection and partial transmission through interface between two media. ....	11
7. Partial reflection and transmission at both boundaries of shield .....	13
8. Multiple reflections in thin shield .....	15
9. Carbon microfiber samples [22].....	17
10. $S_{21}$ measurement setup.....	18
11. Measurement of path loss of air and open aperture.....	19
12. Measured $S_{21}$ for carbon microfiber and aluminum sheets.....	20
13. Stainless steel enclosure for heating / cooling .....	20
14. Measured shielding effectiveness .....	21
15. Dimensions of the heating / cooling measurement setup .....	22
16. Measurement of $S_{21}$ in steel enclosure.....	22
17. Temperature rise measurement inside enclosure .....	23
18. Temperature fall measurement inside enclosure.....	24
19. Horn antenna for simulation.....	25



20.	Radiation pattern of simulated horn antenna.....	26
21.	Simulation setup. ....	27
22.	Simulation and measured $S_{21}$ results for aperture and aluminum sheet..	27
23.	$S_{21}$ simulation results for different fiber conductivities. ....	28
24.	Comparison of $S_{21}$ simulation results for different fiber conductivities. ..	29
25.	Simulated shielding effectiveness for different conductivity values.....	30
26.	Carbon microfiber impedance for 03221 and 03222 from measured $S_{21}$ results.....	31
27.	Analytical shielding effectiveness for different conductivity values. ....	32
28.	Shielding effectiveness comparison of measured, simulated and analytical values. ....	33
29.	Shielding effectiveness comparison for conductivity 2000 $S/m$ .....	34

# LIST OF SYMBOLS

$\omega$	Angular frequency
$f$	Frequency
$\lambda$	Wavelength
$\epsilon$	Permittivity
$\mu$	Permeability
$\mu_r$	Relative permeability
$\sigma$	Conductivity
$\sigma_r$	Relative conductivity
$t$	Thickness (distance inside) of shield
$\delta$	Skin depth
$\Gamma$	Reflection coefficient
$T$	Transmission coefficient
$E$	Electric field
$E_i$	Incident electric field
$E_t$	Transmitted electric field
$E_r$	Reflected electric field
$E_s$	Electric field inside shield
$H$	Magnetic field
$H_i$	Incident magnetic field
$H_t$	Transmitted magnetic field
$H_r$	Reflected magnetic field
$Z_0$	Characteristic impedance of free space
$Z_s$	Shield impedance
$Z_1$	Impedance of medium 1
$Z_2$	Impedance of medium 2

<i>R</i> .....	Reflection loss
<i>A</i> .....	Absorption loss
<i>B</i> .....	Correction factor

# CHAPTER 1. INTRODUCTION & LITERATURE REVIEW

## 1.1. Introduction

There is an ever increasing demand for advanced technology on a daily basis for personal as well as professional use. This use includes not only computer technology, wireless technology, and smart phones, but even use of appliances in the medical field, aircrafts, and food processing. This increasing use of technology produces electromagnetic (EM) induction / electromagnetic radiation denoted as electromagnetic interference (EMI). Electromagnetic shielding is the practice of reducing these EM fields in space by blocking it with a barrier made of magnetic or conductive material. For this work the EM shielding properties of the carbon microfibers shown in Figure 1 for the frequency range 1 *GHz* to 4 *GHz* is investigated. The following two sections present the motivation behind this research work along with an outline for the thesis.

EMI shielding is receiving increasing attention in electronic and communication industries due to increasing sensitivity, density, and abundance of the devices. Composite materials and carbon nanotube structures have been progressively incorporated into large scale manufacturing for lightweight structures for their use in the electromagnetic shielding. The goal of achieving high strength and stiffness while maintaining the low density results in a significant reduction in weight. Carbon microfiber structures are materials that have these light weight properties and are compatible with both economic and environmental concerns.

The most common procedure for protection against EMI is metal shielding. Metals have the potential for eliminating all emissions through absorption and reflection of the waves, thus providing shielding of electronics. However, there is research being conducted on whether lightweight materials like composite materials, carbon nanotubes or carbon microfibers can be sufficient as a replacement for the

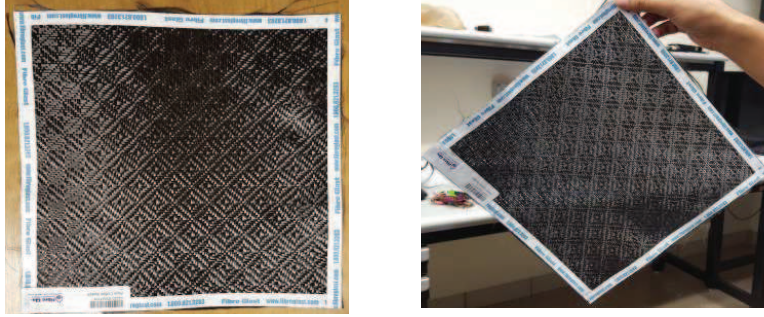


Figure 1. Carbon microfiber sample for shielding

metals. This research is ongoing because metals are expensive, heavier in nature and the verification of the efficiency of these composite materials in the EM shielding is still ongoing. Composite materials and carbon microfibers have made many improvements in terms of weight, cost, and desirable properties. Carbon microfibers have greater elasticity for molding than metals, which allows them to be used in a more versatile manner than metals. These are some of the potential reasons carbon microfibers can be a suitable alternative for metals in EMI shielding.

The EMI in electronic devices is a common problem and if not shielded properly may cause damage to the system. The EMI in medical appliances can cause harm to the person and may restrict the designated apparatus from producing desirable results. The EMI can temporarily disable a piece of technology and if exposed long enough to it without protection could potentially cause permanent damage. So, there is a great need to ensure all electronic devices are properly shielded against the interference. The EMI phenomenon occurs in the frequency ranges from hertz (Hz) to gigahertz (GHz).

Moreover, every circuit element in the devices produces heat when the current flows through it and heat sinks are normally employed to disseminate this heat. This temperature is of concern when the circuit is used in extreme temperature conditions and these conditions can lead to circuit failures. Furthermore, heat sinks

are typically made of metals and are heavy. Additionally, a fan can be used for better dissemination of heat. However, when a metallic shield is used to reduce electromagnetic interference, the circuit is typically completely enclosed. This can then make it difficult to cool a circuit. This research will focus on determining the electrical properties of carbon microfibers, simulation and measurements of the EM shielding. And this research will also consider the heating / cooling effect of using carbon microfiber and a comparison to the metallic enclosures which are conventionally used to house the circuit modules.

Following the introduction, five chapters are presented in this thesis. Here is a short summary of each chapter given.

In this chapter, introduction and motivation of this research work is discussed. This chapter also includes the literature review that has been done in the field of EMI with composite materials. This literature review will focus on the three main areas, carbon nanotubes, non-traditional composites and traditional composites.

Chapter 2 focuses on the theoretical background of EM shielding. The physical mechanism of the EM shielding interference is discussed along with the concept of shielding effectiveness. Explanation and mathematical formulations for absorption, reflection, and multiple reflection / correction factors are elaborated.

In chapter 3, the topic is measurement of the carbon microfiber shielding, but with a complete explanation of carbon microfiber materials and its measurement setup. Carbon microfiber are introduced and their sample numbers are shown. Shielding effectiveness of carbon microfiber samples is discussed followed by the investigation of carbon microfiber sheet for cooling/heating.

In chapter 4, simulations of the carbon microfiber as a shield is discussed along with the details of the simulation setup. This chapter further elaborates on the parametric study of the carbon microfiber shielding for the estimation of conductivity

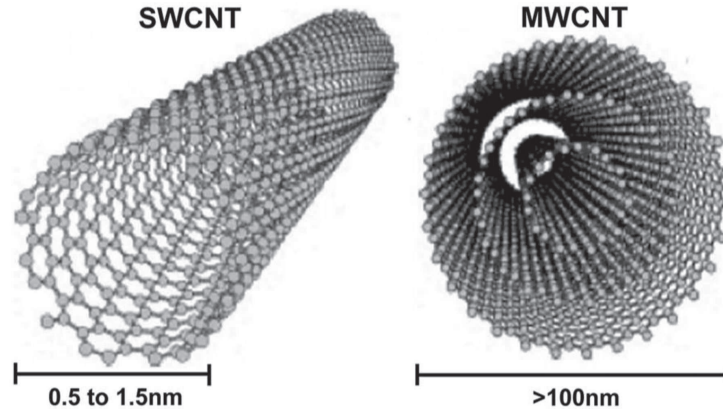


Figure 2. Single wall carbon nanotube and multiwall carbon nanotube [23].

of the material and its reliability of the shielding effectiveness results compared with the measurement results.

Chapter 5 summarizes the results of the analytical formulation of the EM shielding with carbon microfibers using the equations from the literature. Moreover, measurement results, simulation results, and analytical results are compared and discussed in this chapter.

## 1.2. Literature Review

Many composite materials have been used in EM shielding / absorbing applications other than metals and microwave absorbers. These carbon materials for the EMI include composite materials, flexible graphite and colloidal graphite.

### 1.2.1. Carbon nanotubes / nano-fibers

Carbon nano-fibers (shown in Figure 2) is a new form of composites that are being widely used and researched today. Carbon nanotubes (CNTs) are carbon tubes at nano scale and are being investigated for use in many different applications like EMI. CNTs are considered to be the best alternative components for the shielding because they offer better electrical and mechanical properties than conventional composite fillers.

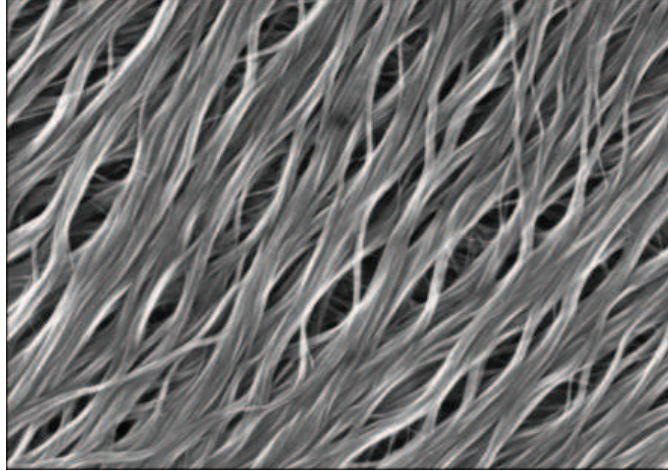


Figure 3. Liquid crystal polymer [24].

Some reported work includes the utilization of liquid crystal polymer (LCP) composites (Figure 3), frequency selective fabric composites, carbon nanotube polymer composites & shape polymer, and carbon nanotube-based composites with polypyrrole fabric for the electromagnetic shielding. In [1], the vapor carbon nanofiber reinforced LCP composites were investigated and the shielding effectiveness (SE) at different frequencies was also studied. These composites were able to exhibit a SE of 41 *dB* having a shielding mechanism of the initial reflection and multiple reflections. Moreover, thermal conductivity of these composite materials showed no enhancement with the introduction of nanofibers.

Due to the skin effect, a composite material having a conductive filler with a small unit size of the filler is more effective than one having a conductive filler with a large unit size of the filler [2]. Polymer matrix composites containing conductive fillers have been used for shielding because of their moldability, this processability helps to reduce seams in the housing that is in the shield [3]- [10]. The seams are considered in the metal shields as they tend to cause radiation leakage and minimize the effectiveness of the shield. In addition, the polymer matrix has a low density and



does not contribute to shielding. However, the polymer matrix effects the connectivity of the conductive filler and thus enhances the shielding effectiveness.

On the other hand, electrical polymers are not common as they are difficult to process and have poor mechanical properties. In [11]- [12], multi-wall nano tubes fill glass / epoxy plain weave and carbon nanotube reinforced composites are investigated for absorption of electromagnetic signals thus reducing the radar cross sectional area to be used in aerospace applications. The main disadvantage of carbon fiber composite material is normally its low conductivity and thus low shielding effectiveness.

Metals are more attractive candidates for shielding than carbon polymers and nanotubes due to their high conductivity. But there are also some disadvantages associated with the utilization of metal mainly for shielding purposes such as high weight, increased cost, poor corrosion resistance, poor thermal properties, and rigidity. These drawbacks have influenced designers to find suitable alternatives to the metals and many composite materials have been proposed in this regard [13]- [16]. On the other hand, carbon fibers have the advantage of having oxidation resistance and thermal stability. References [11], [12] and [17] give some of the shielded effectiveness values at  $1 - 2 \text{ GHz}$  for polyethersulfone (PES) matrix composites with various fillers.

### **1.2.2. Flexible graphite and colloidal graphite for shielding**

A flexible graphite (Figure 4) is a flexible sheet that is made by compressing a collection of exfoliated graphite flakes (worms) without a binder. The electrical conductivity and specific surface area are quite high in flexible graphite, which results in the shielding effectiveness to be very high (i.e. up to  $130 \text{ dB}$  at  $1 \text{ GHz}$  [17]).

Colloidal graphite is the combination of graphite powder suspended in liquid (water/alcohol) with a small amount of polymer binder. This mixture is then applied to a surface by painting or other means, the liquid carrier evaporates, thus resulting

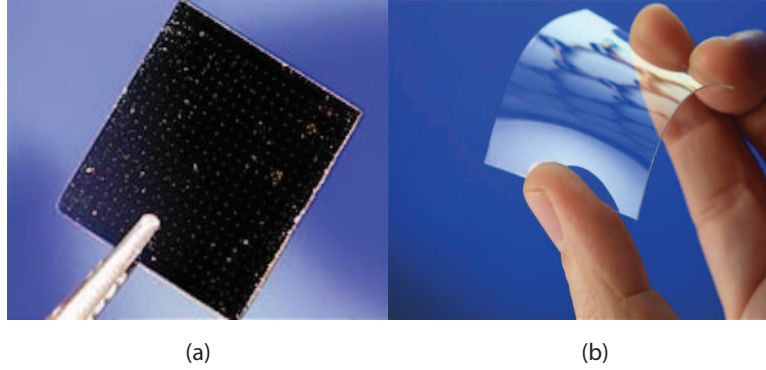


Figure 4. Graphite material [25] (a) Single carbon atom  
(b) Flexible graphene material

in the graphite particles to be in the direct contact on that surface. This coating is effective for EMI shielding.

### 1.3. Conclusions

All of the literature reviewed has its importance for the EMI shielding community using composites and carbon materials. Carbon materials used for EMI shielding are carbon fiber composites, LCP, flexible graphite, and colloidal graphite. The formation types of these composites include non-structural with discontinuous fibers and structural with continuous fibers. However the main disadvantage of these carbon materials is normally their low conductivity and thus low shielding effectiveness. EM shielding of carbon microfiber samples has not been explored yet, though these woven structures have conductivity, have light weight and are flexible. This research work is related to the detailed electromagnetic shielding effectiveness of carbon microfiber samples and simulation setup reliability for EMI shielding. Moreover, the heating / cooling properties of the carbon microfibers are measured in the metallic enclosure and are then compared with the metallic sheet. Based on the measurement results, simulations in HFSS v 15.0 [15] are carried out for utilizing the carbon microfiber for shielding purposes. The simulation results are then validated through measurement.

A parametric study on the conductivity of the carbon microfiber is performed, and S-parameters results are compared with that of the measurement results thus confirming the reliability of the simulation model.

## CHAPTER 2. THEORY OF ELECTROMAGNETIC SHIELDING

A shield is basically a partition, normally metal in the space between two regions. The purpose of this metallic shield is to isolate these two regions electromagnetically (i.e., the propagation of electromagnetic waves ceases between these two regions because of this metallic shield). The metallic shield can be used in two configurations. One is to contain the source in the shield so that the electromagnetic field does not go out. And the other way is to protect the specific receiver/equipment with the shield so that the electromagnetic field does not interfere with it. Both the configurations are shown in the Figure 5.

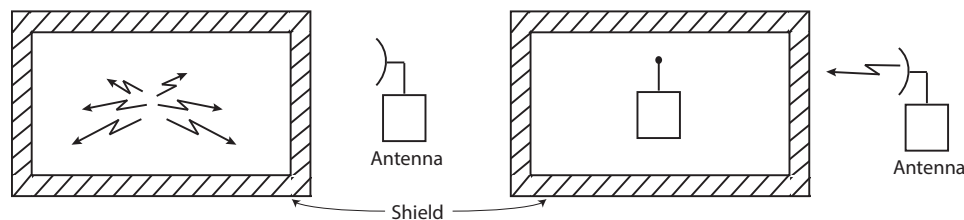


Figure 5. Shielding application for shielded source and receptor.

Now the electromagnetic field's characteristics are dependent on the source, the media surrounding it and the distance from the source. Near to the source, the characteristics are dependent on the source and, as we go far from the source, the characteristics of the electromagnetic field mainly depends on the medium through which the wave is propagating. So we can divide the medium around the source into two regions namely near-field and far-field. If the distance from the source is less than  $\lambda/2\pi$  then we are in near-field region and if the distance is greater than  $\lambda/2\pi$  than we are in far-field region [20].

## 2.1. Wave Impedance

The wave impedance is defined as the ratio of the electric field (E) to the magnetic field (H) and is written as [20]:

$$Z_W = E/H \quad (2.1)$$

whereas the characteristic impedance of the medium is defined as [21]:

$$Z_0 = \sqrt{\frac{j\omega\mu}{\sigma + j\omega\epsilon}}. \quad (2.2)$$

For the case of a plane wave (i.e., far-field region),  $Z_0$  is also equal to the wave impedance  $Z_W$ . And for insulators,  $\sigma \ll j\omega\epsilon$  and this equation reduces to [20]:

$$Z_0 = \sqrt{\frac{\mu}{\epsilon}} \quad (2.3)$$

For the case of conductors with  $\sigma \gg j\omega\epsilon$ , the characteristic impedance is also called the shield impedance and is written as [20]:

$$Z_s = \sqrt{\frac{j\omega\mu}{\sigma}} = \sqrt{\frac{j\omega\mu}{2\sigma}}(1 + j) \quad (2.4)$$

or

$$|Z_S| = \left| \sqrt{\frac{j\omega\mu}{2\sigma}} \right|. \quad (2.5)$$

For any conductor, in general:

$$|Z_S| = 3.368 \times 10^{-7} \sqrt{\frac{\mu_r f}{\sigma_r}}. \quad (2.6)$$

The relative values are with respect to copper for which  $\sigma = 5.8 \times 10^7 \text{ S/m}$  and  $\mu = 4\pi \times 10^{-7} \text{ H/m}$ .

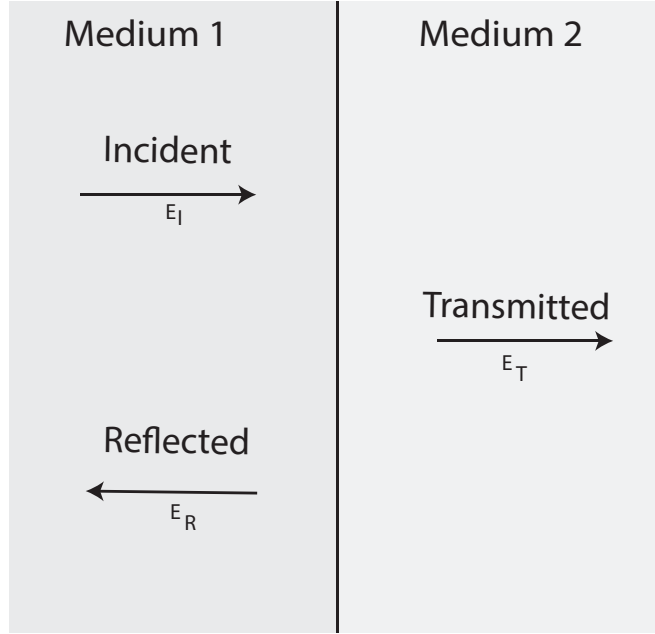


Figure 6. Partial reflection and partial transmission through interface between two media.

## 2.2. Shielding Effectiveness

Shielding effectiveness is defined as:

$$SE = 20 \log \frac{E_i}{E_t} = 20 \log \frac{H_i}{H_t} \quad (2.7)$$

where ‘i’ denotes the incident field and ‘t’ denotes the transmitted field. The shielding effectiveness for a metallic sheet mainly comprises of two portions. One is the reflection from the surface which is called the reflection loss and is dependent on the type of field and the wave impedance. The second is the attenuation of the wave inside the shield as the transmitted (non-reflected) wave passes through it. This is called the absorption loss and this mainly depends on the skin depth and the thickness of the shield. So we can write the total shielding effectiveness of the solid material shield as:

$$SE = R + A + B(dB) \quad (2.8)$$

where R is the reflection loss, A is the absorption loss and B is the correction factor which accounts for the multiple reflections in thin shields.

### 2.3. Reflection Loss

Now for the case of reflection, consider the following simple case as shown in Figure 6.  $E_i$  is the electric field intensity of the incident electromagnetic wave at the boundary of the medium 1 and medium 2.  $E_t$  is electric field intensity of the transmitted electromagnetic wave from medium 1 to medium 2 and  $E_r$  is the Electric field intensity of the reflected electromagnetic wave from the junction of medium 1 and medium 2 to medium 1. The reflection coefficient can be written as:

$$\Gamma = \frac{Z_2 - Z_1}{Z_2 + Z_1} \quad (2.9)$$

and the transmission coefficient can be written as:

$$T = 1 - \frac{Z_2 - Z_1}{Z_2 + Z_1} = \frac{2Z_1}{Z_1 + Z_2}. \quad (2.10)$$

Then

$$E_t = TE_i = \frac{2Z_1}{Z_1 + Z_2} E_i \quad (2.11)$$

Next, consider the set up for the shielding measurement as shown in Figure 7, and applying these concepts.

$E_i$  is the incident wave at shield from medium 1 (air)

$E_s$  is the wave transmitted inside the shield through boundary 1

$E_T$  is the transmitted wave from shield to medium 2 (air)

$T_s$  is the transmission coefficient between shield and medium 1

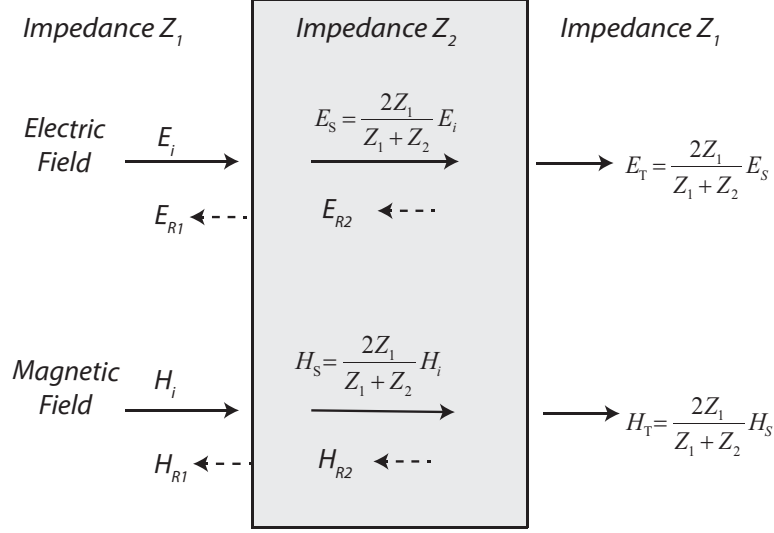


Figure 7. Partial reflection and transmission at both boundaries of shield

and  $T$  is the transmission coefficient between shield and medium 2.

Now the electric field intensity inside the shield is written as:

$$E_s = TE_i = \frac{2Z_q}{Z_1 + Z_s} E_i \quad (2.12)$$

and the transmitted electric field through the shield can be written as:

$$E_t = TE_s = \frac{2Z_s}{Z_1 + Z_s} E_s \quad (2.13)$$

or

$$E_t = \frac{2Z_s}{Z_1 + Z_s} \frac{2Z_1}{Z_1 + Z_s} E_i = \frac{4Z_1 Z_s}{Z_1 + Z_s^2} E_i. \quad (2.14)$$

For a plane wave the impedance of air is  $Z_1 = 377 \Omega$  and for conductors  $Z_s \ll Z_1$ , so

$$E_t = \frac{4Z_s}{Z_i} E_i. \quad (2.15)$$



Now defining the reflection loss as:

$$R = 20 \log \frac{E_i}{E_t} = 20 \log \frac{377}{4Z_s} \quad (2.16)$$

and using the value of shield impedance, we get the equation for the reflection loss as:

$$R = 168 + \log \left( \frac{\sigma_r}{\mu_r f} \right) dB. \quad (2.17)$$

## 2.4. Absorption Loss

The amplitude of the electromagnetic wave decreases exponentially as it passes through the medium. This happens because the induced currents in the shield (medium) produce ohmic losses and thus heating of the shield material. Therefore we can write:

$$E(H)_1 = E(H)_0 e^{-\frac{t}{\delta}} \quad (2.18)$$

where  $E(H)_1$  is the field intensity at a distance 't' inside the shield and  $E(H)_0$  is the incident field intensity on the shield. 'δ' is the skin depth which can be defined as the distance required for the field to be attenuated to  $\frac{1}{e}$  or 37% of its value and can be written as:

$$\delta = \sqrt{\frac{2}{\omega \mu \sigma}} m = \sqrt{\frac{2.6}{f \mu_r \sigma_r}} in \quad (2.19)$$

where  $\mu_r, \sigma_r$  are the relative permeability and relative conductivity with respect to copper.

Now we can write the absorption loss through the shield as:

$$A = 20 \log \frac{E_0}{E_1} = 20 \log e^{\frac{t}{\delta}} \quad (2.20)$$

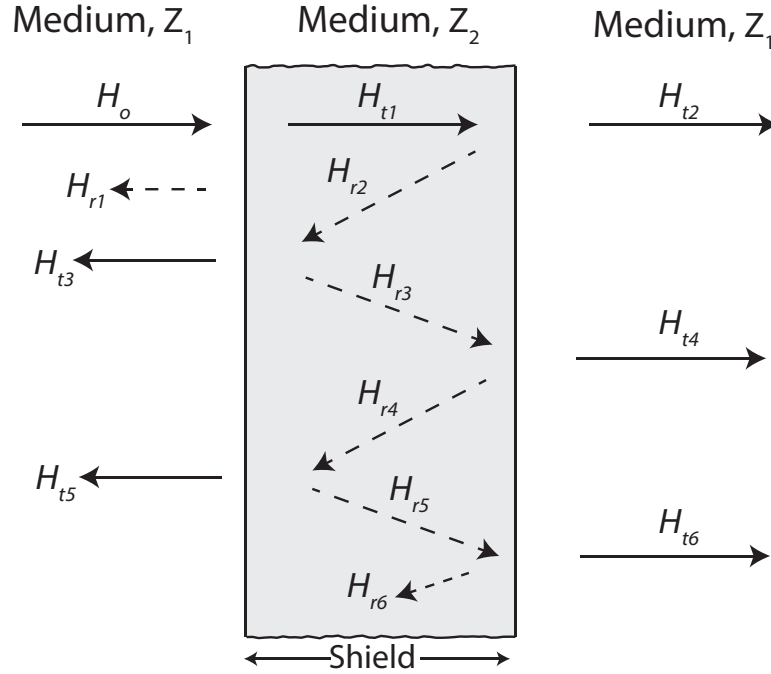


Figure 8. Multiple reflections in thin shield

and

$$A = 8.69 \left( \frac{t}{\delta} \right) dB \quad (2.21)$$

Putting the expression for skin depth in the equation then gives:

$$A = 3.34t \sqrt{f \mu_r \sigma_r} dB \quad (2.22)$$

where 't' is the thickness of the shield.

## 2.5. Correction Factor / Multiple Reflections in Thin Shield

If the shield is thin, then the electromagnetic wave inside the shield is reflected back from the second boundary and is incident upon the first boundary. Here some of this wave is transmitted through the first boundary towards the original source and the rest of the wave is reflected back to the second boundary either to transmit to the receiver or to reflect again inside the shield as shown in Figure 8.

For the case of the electric field, most of the field is reflected from the first boundary as  $Z_2 \ll Z_1$ . Therefore, multiple reflections can be neglected for the electric field. For the case of the magnetic field, most of the wave passes through the first boundary of the shield as  $Z_2 \ll Z_1$ . Therefore the effect of multiple reflections needs to be considered for the magnetic field. The correction factor for the case of the magnetic field is:

$$B = 20 \log \left( 1 - e^{-\frac{2t}{\delta}} \right) dB \quad (2.23)$$

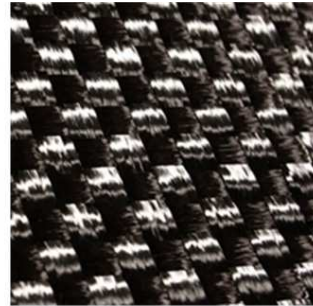
where 't' is the thickness and ' $\delta$ ' is the skin depth for the shield.

## CHAPTER 3. MEASUREMENTS

The carbon microfiber samples used for this study were the 24k carbon tow from fiberglast shown in Figure 9. These tows are composed of filaments of diameter  $7 \mu m$  and are composed of 24000 filaments with a tensile strength of  $710 - 750 \text{ ksi}$ . This carbon fiber is used in four different woven patterns for this study.



Part # 3220 by Fiber Glast™



Part # 3221 by Fiber Glast™



Part # 3222 by Fiber Glast™



Part # 3223 by Fiber Glast™

Figure 9. Carbon microfiber samples [22].

To utilize the carbon microfiber as a shielding material, we assembled the set up in Figure 10 with a  $61 \text{ cm} \times 91 \text{ cm}$  aluminum sheet with a thickness of  $0.32 \text{ cm}$ . This sheet was cut from the center with the dimension  $28 \text{ cm} \times 28 \text{ cm}$  making an aperture in the center of the sheet. The dimensions of the aperture were a little less than the size of the carbon microfiber samples as the size of the samples was  $30 \text{ cm} \times 30 \text{ cm}$ . Then we used the *TDK - HRN - 0118* horn antennas as transmitter

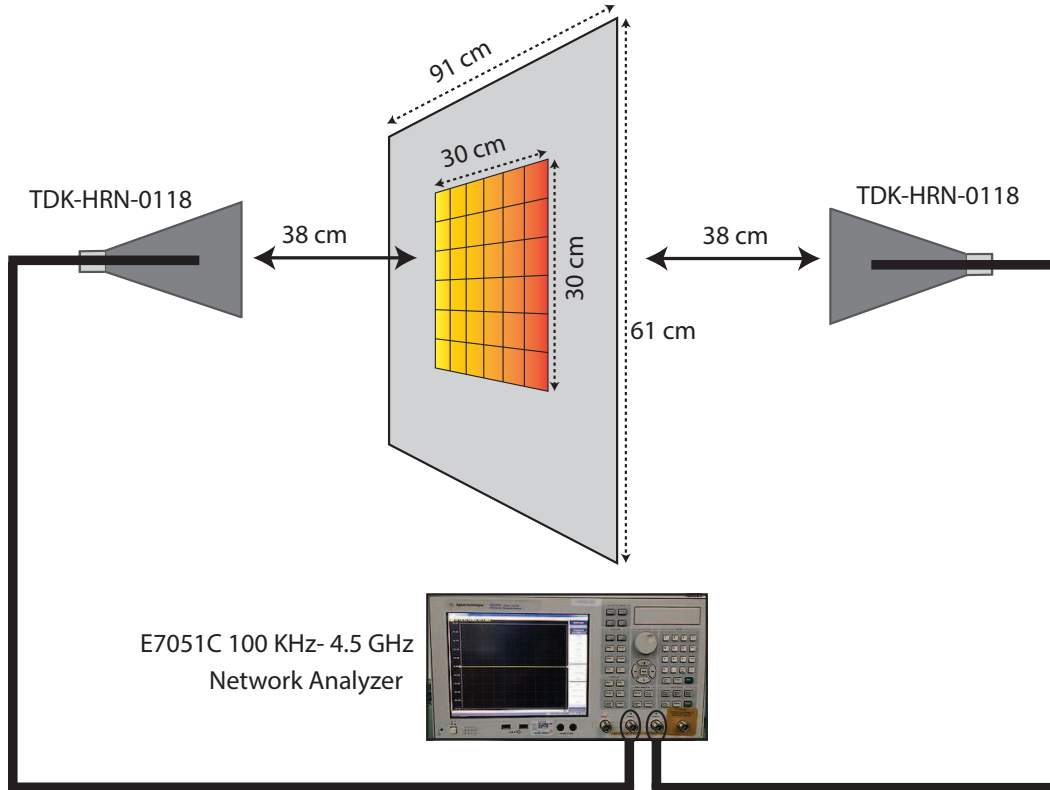


Figure 10.  $S_{21}$  measurement setup.

and receiver pair, and the distance between these two antennas was 76 *cm*. These antennas are designed for the frequency range 1 – 18 *GHz*. The network analyzer used for measurement in this set up was an Agilent *E5071C* 100 *kHz* – 4.5 *GHz* ENA series network analyzer. We chose the frequency range for the measurements from 1 *GHz* to 4 *GHz*.

Next, we compared the measurements of the two scenarios. One was that there was nothing in between the antennas, and only the path loss was occurring between the antennas for the measurement of  $S_{21}$ . The other scenario was that the aluminum sheet with the cut aperture was put in the middle, and then these measurements were repeated. These measurements are shown in Figure 11. As we can observe from the measurements that both of these measurements are pretty close to each other, i.e.,

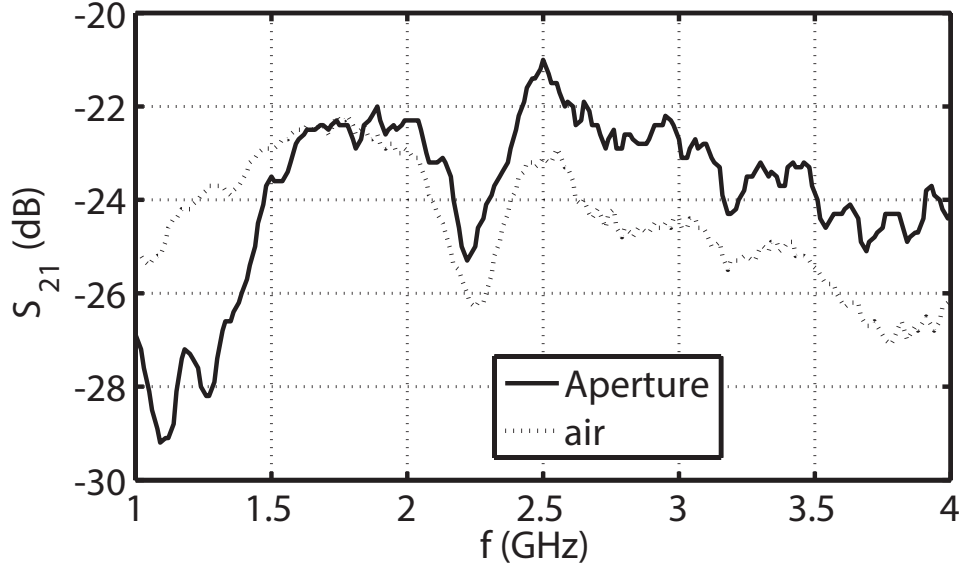


Figure 11. Measurement of path loss of air and open aperture

only a 1 – 2  $dB$  difference. There was only one contradiction to this measurement at the frequency of 1.1  $GHz$  where the difference between the measurements in 4  $dB$ . Overall we can say that the horn antennas are directing the waves through the aperture.

The next step in the measurements was to cover the aperture with the samples and measure  $S_{21}$ . This measured  $S_{21}$  should be very much less than  $S_{21}$  measured earlier with nothing between the antennas and the  $S_{21}$  of the aluminum sheet with the aperture between the antennas due to the fact that the carbon microfiber is shielding the signal. Also we covered the aperture with an aluminum sheet and made the measurement for reference.

These measurement results are shown in the Figure 12, and we can observe from the figure that the  $S_{21}$  values for all the four samples of carbon microfiber in Figure 9 are in close agreement to each other. Thus we can deduce that the aluminum sheet and the carbon microfiber is allowing almost the same amount of signal to

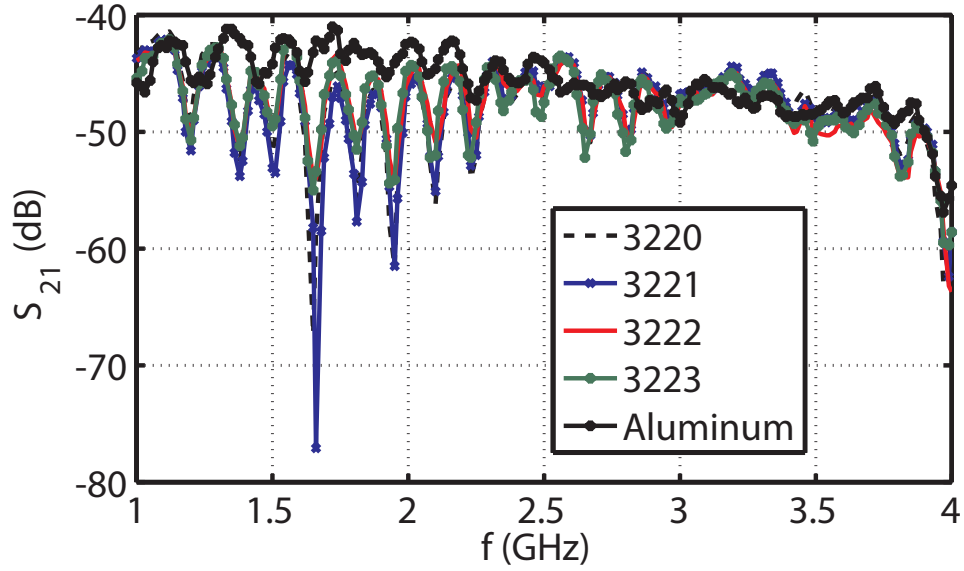


Figure 12. Measured  $S_{21}$  for carbon microfiber and aluminum sheets

pass through them or in fact, the carbon microfiber has a shielding similar to a solid aluminum sheet.

Next, we translated this measured  $S_{21}$  to shielding effectiveness (SE). For this we need to take into account the path loss which occurred between the two antennas as we can not take this loss as shielding. So we deducted the path loss earlier measured

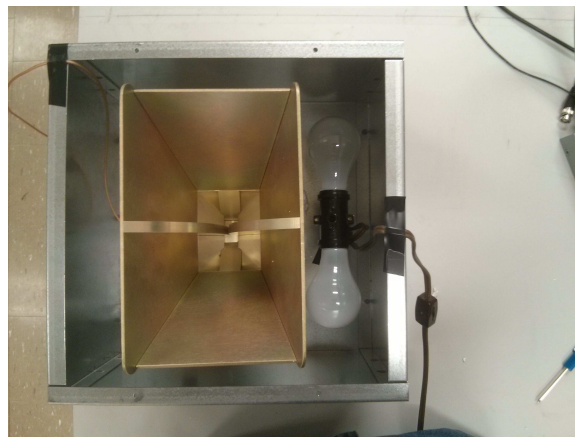


Figure 13. Stainless steel enclosure for heating / cooling

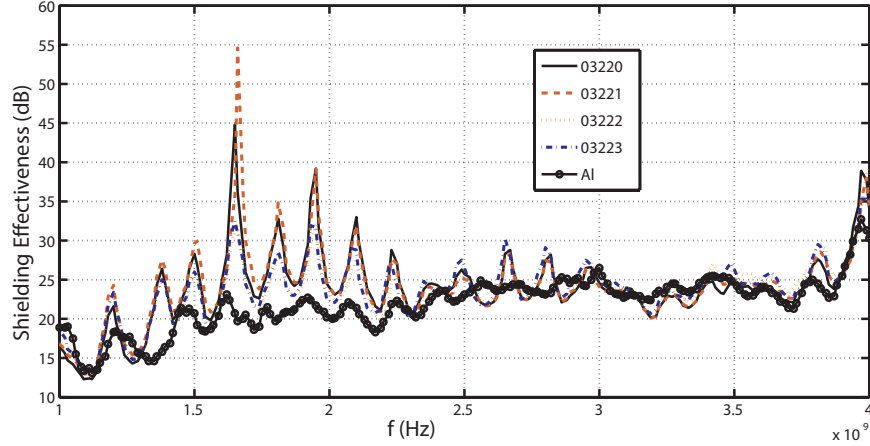


Figure 14. Measured shielding effectiveness

from this  $S_{21}$  measurement for the carbon microfiber and aluminum and plotted the shielding effectiveness in Figure 14. As we can see from the plot that all the SE values for the four samples of carbon microfiber follow each other thus depicting that the woven pattern does not effect the shielding effectiveness. Also the shielding from the aluminum is following the graphs from the carbon microfiber with the only difference that it is lower by 2 – 3  $dB$  in some instances. Overall the shielding effectiveness is the same as the conducting aluminum sheet.

The next setup which we used for both the heating / cooling testing and shielding is shown in Figure 13 . This setup consisted of a stainless steel metallic box of size  $30.5\text{ cm} \times 30.5\text{ cm}$  with a height of  $41\text{ cm}$ . The top plate of the metallic enclosure was cut to give it the opening / aperture so that the shielding for the stainless steel and the carbon microfiber could be measured and compared.

One horn antenna was placed inside the steel enclosure facing out towards the aperture and the other antenna was placed on the top outside of the enclosure at a distance of  $76\text{ cm}$  as shown in Figure 15. Then we measured  $S_{21}$  with the aperture covered with the metallic stainless steel sheet and the carbon microfiber samples. The measured results are shown in the Figure 16. It can be observed from the results



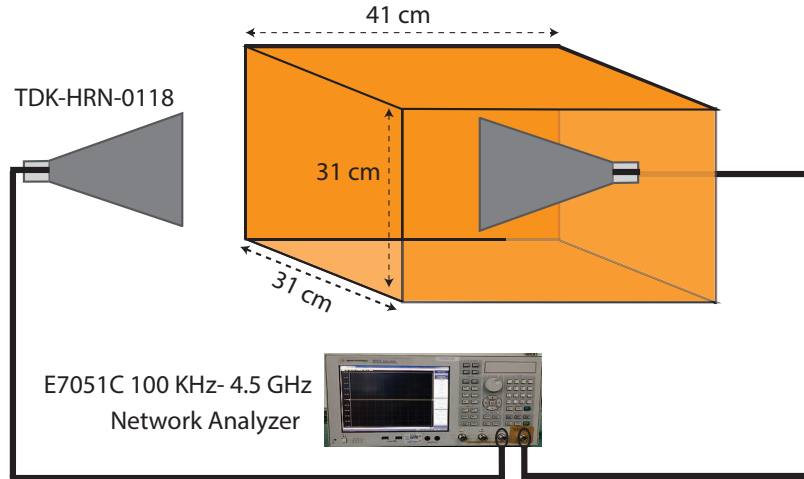


Figure 15. Dimensions of the heating / cooling measurement setup

that the shielding from the stainless steel and the carbon microfiber samples are in close agreement throughout the frequency range of 1 GHz to 4 GHz. It can also be deduced that a similar shielding effectiveness is observed for all samples.

This same setup is used to test the thermal properties of the carbon microfiber and steel covering the aperture of the enclosure. Two 100 W bulbs were used inside

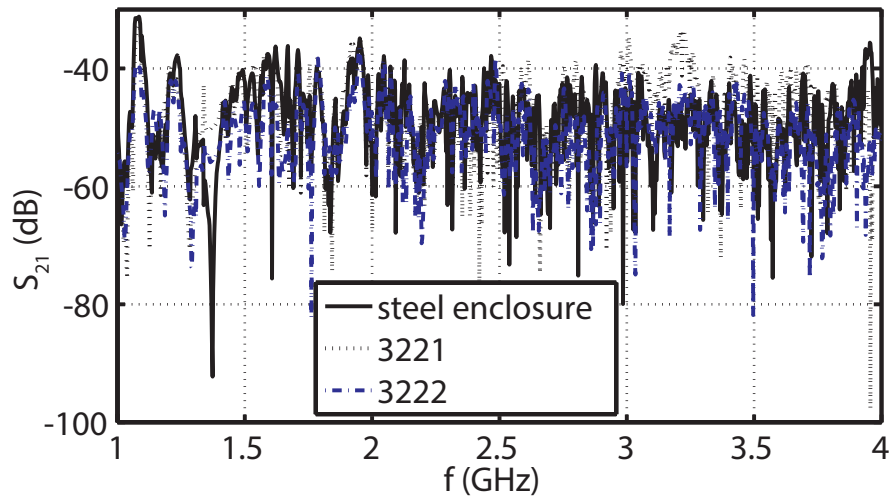


Figure 16. Measurement of  $S_{21}$  in steel enclosure

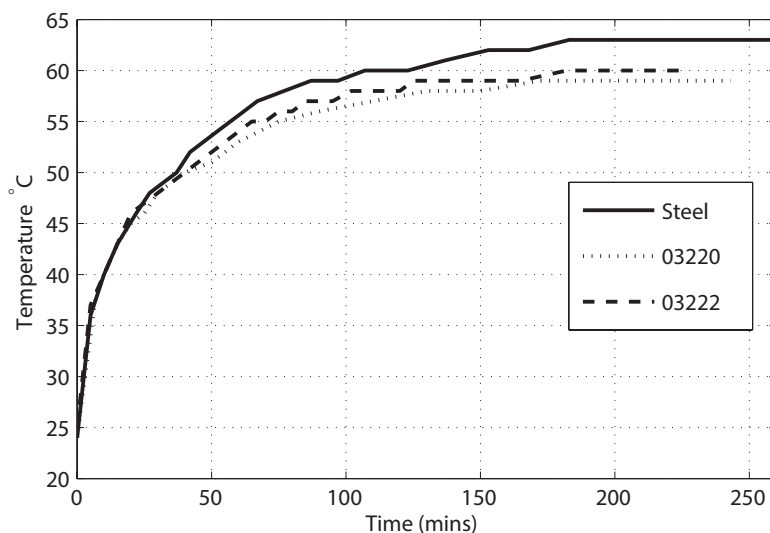


Figure 17. Temperature rise measurement inside enclosure

the enclosure to generate the heat, and the temperature was measured over time. Figure 17 shows the temperature rise with respect to time and it can be seen that the temperature in the steel covered enclosure rises earlier than the carbon microfiber covered enclosure above 45°C. Also the maximum temperature for the carbon microfiber covered enclosure was 5°C less than the steel covered enclosure.

The temperature fall time for this setup was also measured and is shown in the Figure 18. Though the time to reach the room temperature was almost the same for both the cases, the decrease in temperature from the highest point to almost 30°C was faster in the carbon microfiber covered enclosure. Thus it can be said that the operating temperature inside the carbon microfiber covered enclosure is always less.  $S_{21}$  was also measured during these heat/cool cycles but there was no observable difference in the measurement.

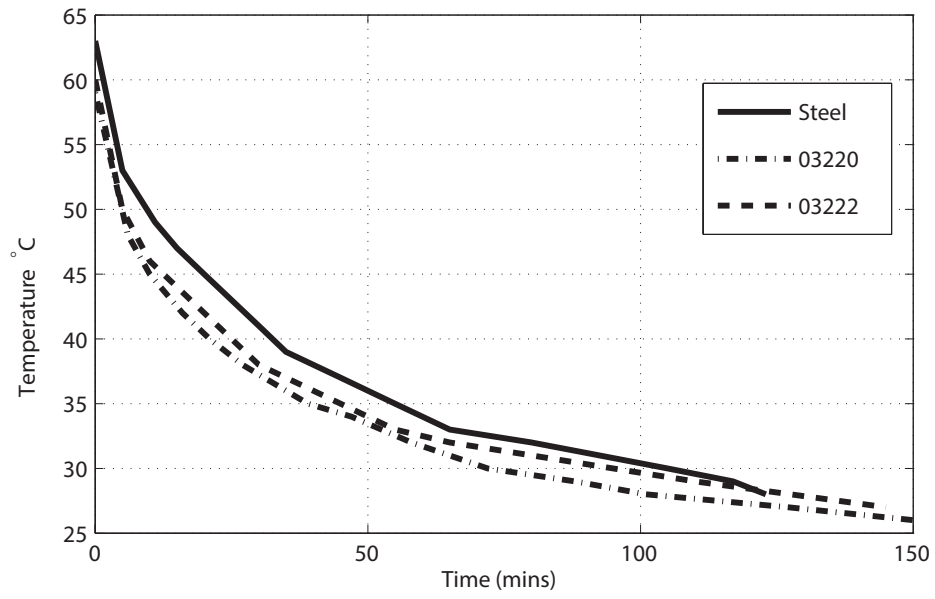


Figure 18. Temperature fall measurement inside enclosure

## CHAPTER 4. SIMULATION OF CARBON MICROFIBER SHIELD

In a previous chapter we discussed the details about the measurement setup and the results we get from our shield. In this chapter we will simulate the environment in the simulation software for electromagnetic, namely, High Frequency Simulation Software (HFSS) 15.0 and will match the environment and the measurements with the simulation. This chapter describes the steps to achieve this goal.

### 4.1. Simulation Setup

For simulation purposes, the actual measurement environment is incorporated in the design of the simulation. First, the actual horn antenna with the dimensions  $width = 23.4\text{ cm}$ ,  $depth = 29\text{ cm}$  and  $height = 14.5\text{ cm}$  is simulated as shown in the Figure 19. The material of the antenna is aluminum and the thickness of aluminum is  $0.32\text{ cm}$ . The actual *TDK – HRN – 0118* antenna is designed for the frequency range

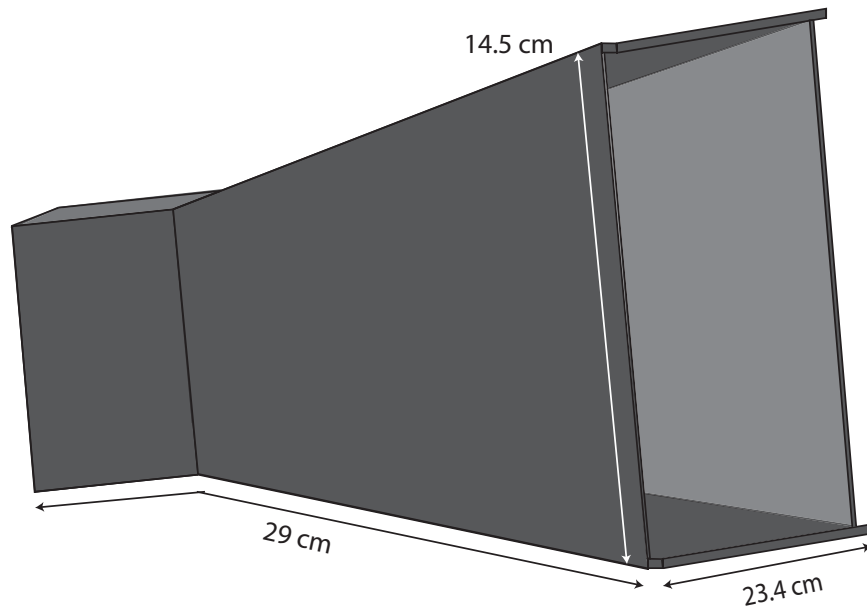


Figure 19. Horn antenna for simulation.

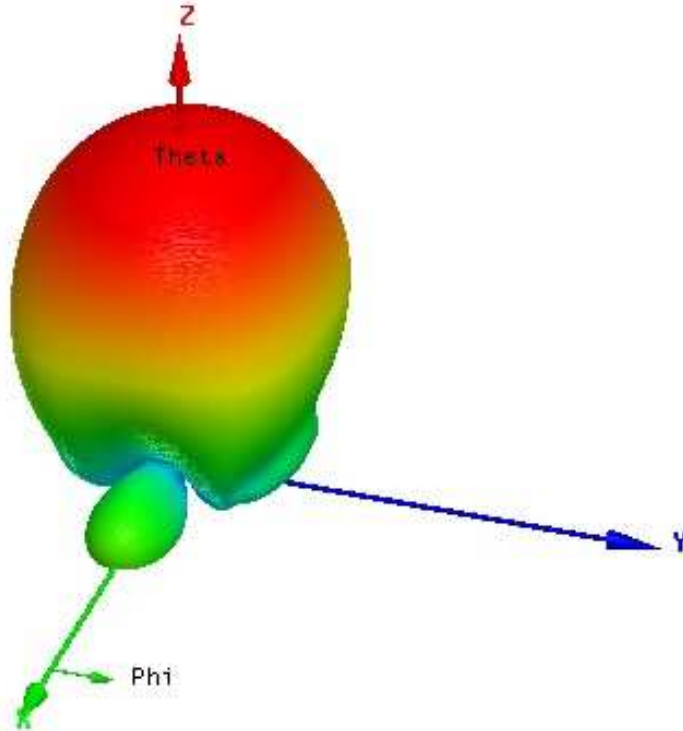


Figure 20. Radiation pattern of simulated horn antenna.

from 1 GHz to 18 GHz. But we simulated the antenna only for the frequency range from 1 GHz to 4 GHz as our measurements are only in this frequency range. The simulation results for the horn antenna are shown in Figure 20. These simulations are in agreement with the actual antenna specifications as provided by the manufacturer in the data sheet.

Then we simulated our actual measurement setup by placing two horn antennas as transmitter and receiver in the simulation setup at a distance of 76 cm as shown in Figure 21. Both of these antennas are driven by wave ports with one antenna as a transmitter (source) and the other antenna as a receiver. Also the aluminum sheet is placed at the center (i.e., at 38 cm from both the transmitter and receiver antenna). The sheet is cut from the center with the dimension 28 cm  $\times$  28 cm to make an aperture at the center, as used in the measurement. The air box containing this

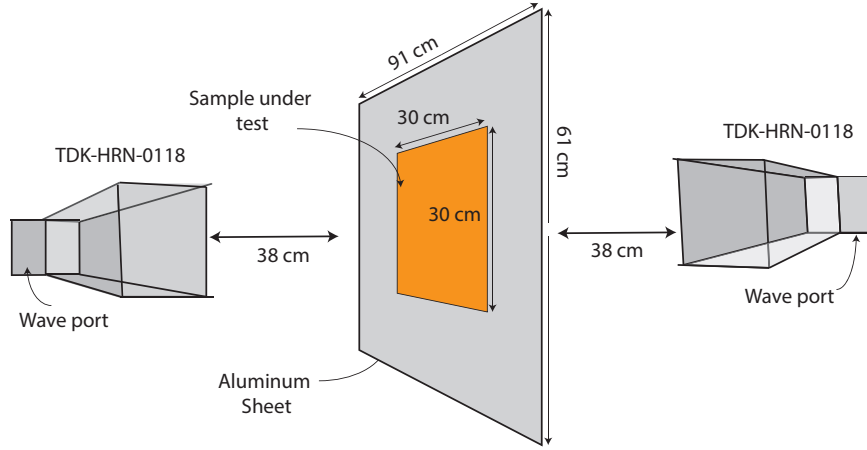


Figure 21. Simulation setup.

setup was of size  $91.5\text{ cm} \times 117\text{ cm} \times 132\text{ cm}$ , and this air box was assigned with radiation boundary conditions.

#### 4.2. Measurement Results

Then we simulated this setup by covering the aperture both with aluminum and microfiber. The simulation results with the aperture covered with aluminum are

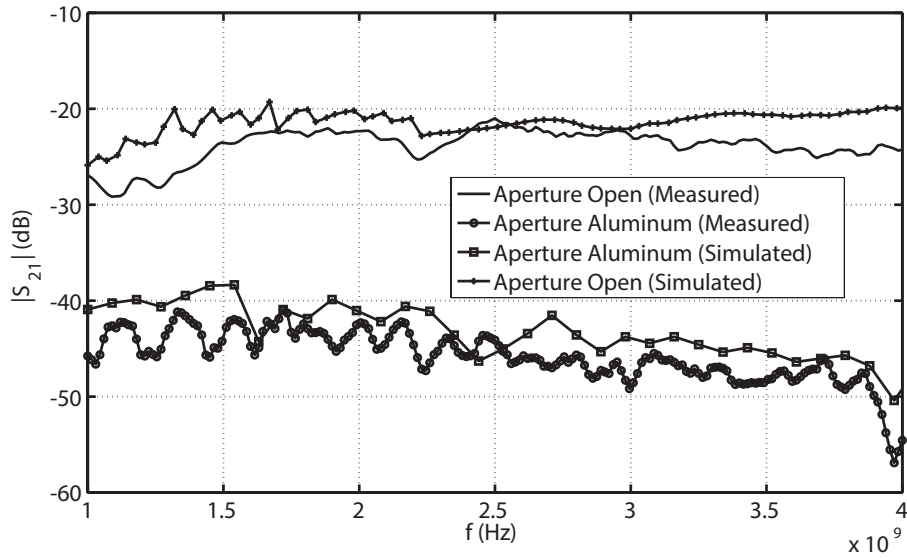


Figure 22. Simulation and measured  $S_{21}$  results for aperture and aluminum sheet.

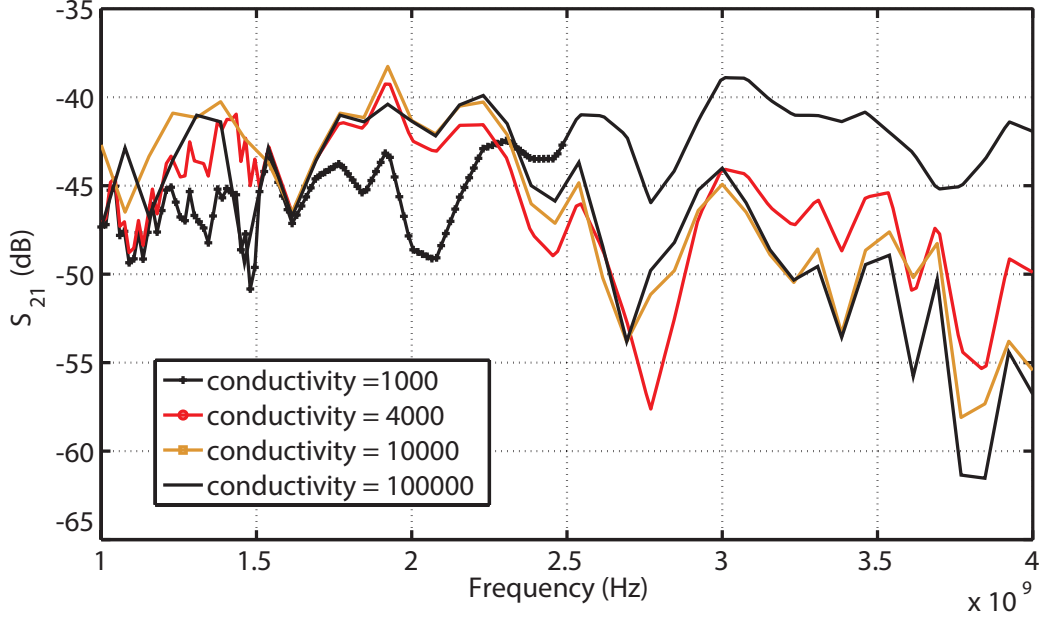


Figure 23.  $S_{21}$  simulation results for different fiber conductivities.

similar to the measured results, i.e., the transmitted signal  $S_{21}$  for the measured and simulated environment are in agreement. The  $S_{21}$  results for the simulation are shown in the Figure 22.

The simulation and measured results show that there is approximately a 2–3 *dB* difference for the frequency range and both the results follow each other very closely. This agreement between these results shows that the simulation environments we are considering for this project are reliable and a good approximation.

Next, we simulated the environment with the microfiber sheet at the center covering the aperture. For this purpose, we assumed carbon microfiber as a solid sheet as the gaps between woven pattern are very small, and it is equivalent to a flat sheet. The relative permeability  $\mu_r$  for carbon microfiber is 1 as it is not a magnetic material. Also as the electrical property (conductivity) of the carbon microfiber material is unknown, so we did the parametric simulation for the environment with

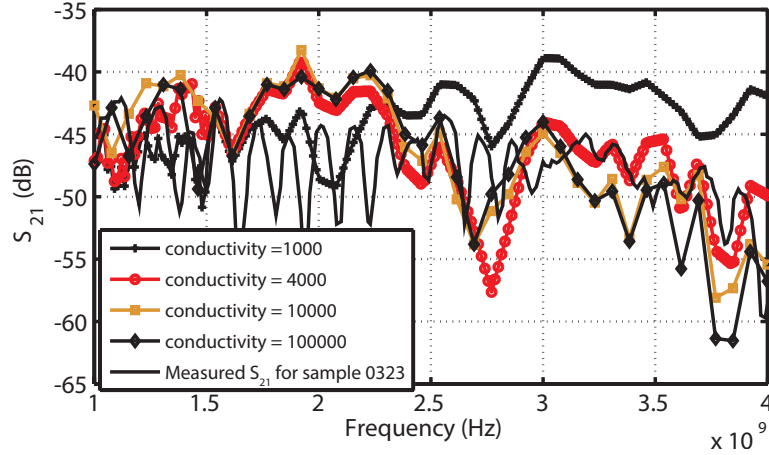


Figure 24. Comparison of  $S_{21}$  simulation results for different fiber conductivities.

conductivity as the variable. The idea is that the shielding effectiveness depends on the material property conductivity, so the simulated  $S_{21}$  values should be different for different conductivity values. Utilizing this idea we did the simulation for the value of conductivity from  $100 \text{ S/m}$  to  $10^7 \text{ S/m}$ . The  $S_{21}$  results for different values of conductivity are shown in the Figure 23. Note that not all the simulation results are shown to decrease the clutter in the plot.

These  $S_{21}$  results were then compared to the measured  $S_{21}$  results. By this comparison, we estimated the value of conductivity for the carbon microfiber. To further strengthen this deduction of carbon microfiber conductivity, the comparison of these measured and simulated results with the analytical shielding effectiveness values for this conductivity is presented in the next chapter. Here the closest results are compared to carbon microfiber sample 0323 and are shown in the Figure 24. The  $S_{21}$  values for these simulations remain almost the same for the higher conductivity values. In the  $10^4$  range, the  $S_{21}$  values start to decrease meaning a decrease in the shielding. Here the comparison of the measured  $S_{21}$  values of sample 0323 with four different conductivities is done.



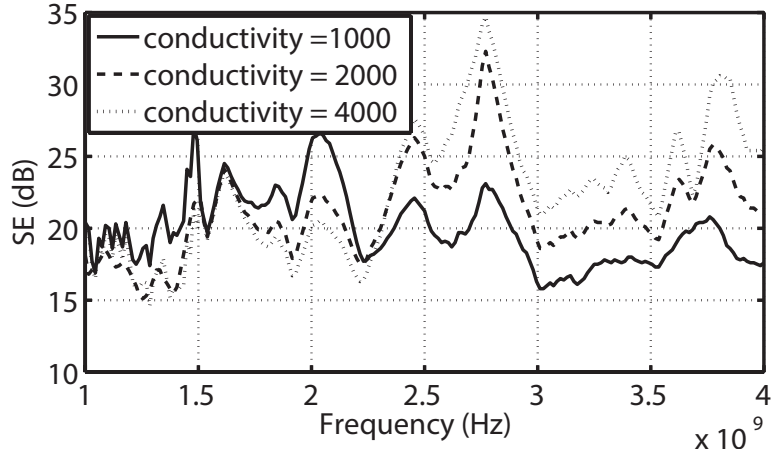


Figure 25. Simulated shielding effectiveness for different conductivity values.

To convert these  $S_{21}$  values, we need to consider the path loss effect for this setup. The  $S_{21}$  values for the aperture case are used for evaluating the shielding effectiveness. The  $S_{21}$  values for the open aperture are in agreement with the values of  $S_{21}$  without any sheet between the transmitter and receiver antennas and the analytical value for path loss. The shielding effectiveness for the simulation case is shown in the Figure 25.

## CHAPTER 5. ANALYTICAL FORMULATION AND COMPARISON OF RESULTS

For analytical shielding calculations, the theory as described in Chapter 2 is used to calculate the analytical shielding for the carbon microfiber. For this purpose, the carbon microfiber's woven structure is assumed as a plain sheet. Thus the equations derived previously are utilized to calculate the shielding effectiveness analytically for the operating frequency range of 1 GHz to 4 GHz.

The conductivity of the material is unknown, so we used simulation results and calculated the shielding for different conductivity values whose  $S_{21}$  values were in agreement with the measured results. For the purpose of calculating the analytical shielding, we are taking into account the reflection loss of electromagnetic shielding. The absorption loss (A) and correction factor (B) are neglected for this particular case because of the thin nature of the carbon microfiber material.

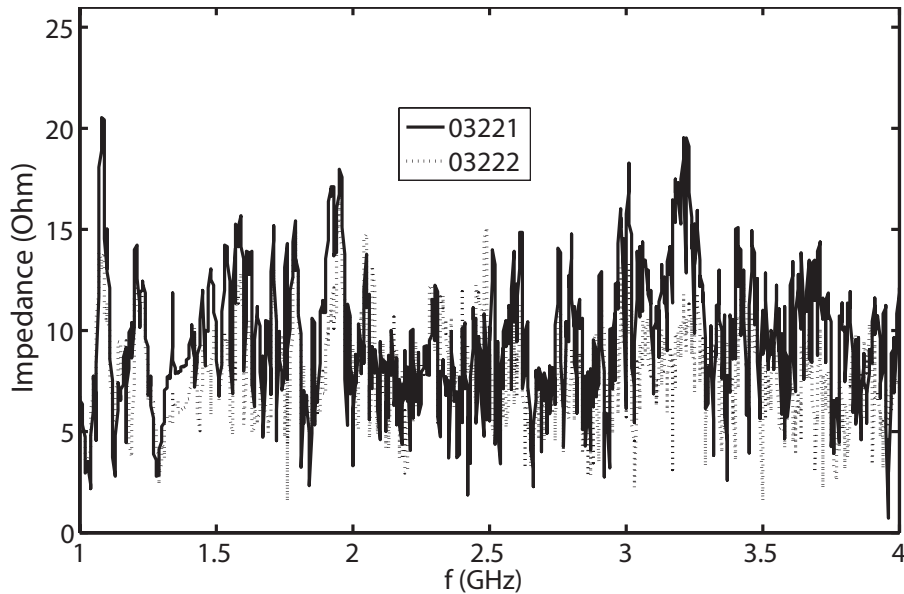


Figure 26. Carbon microfiber impedance for 03221 and 03222 from measured  $S_{21}$  results.

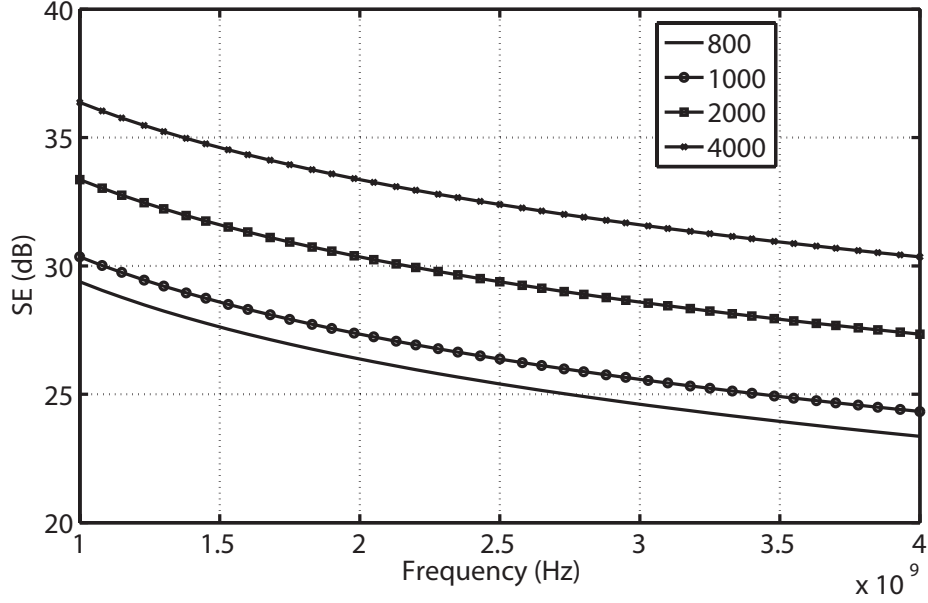


Figure 27. Analytical shielding effectiveness for different conductivity values.

The reason for neglecting the absorption loss (A) is that it has a diameter of  $7 \mu m$  for single filament which is comparable to the skin depth of the signal. Thus we can ignore the absorption loss as the signal does not effectively propagate inside the material for a sufficient distance for absorption loss to be of a significant value. Also the impedance value of the medium (carbon microfiber) is quite low in comparison to the free space impedance as calculated from the measured  $S_{21}$  results and is shown in the Figure 26.

Thus the main shielding happens due to reflection on the first boundary as in a metallic shield. The correction factor is only needed for the case of the magnetic field where the reflection happens at the second boundary. We can ignore the term B for a plane wave and for the electric field because of high reflection loss and very small correction factor. Thus the analytical shielding results for different conductivity values are calculated and they only comprise of the reflection loss. These results are shown in Figure 27.

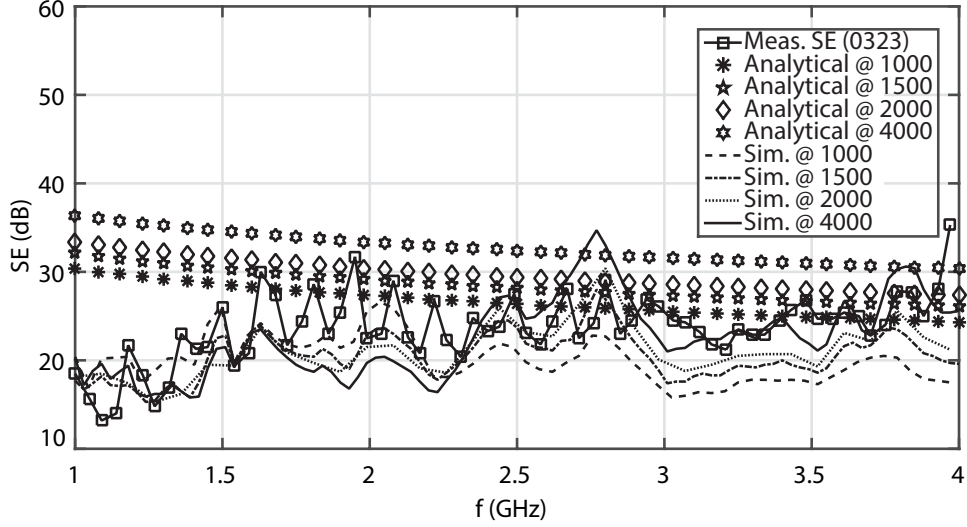


Figure 28. Shielding effectiveness comparison of measured, simulated and analytical values.

### 5.1. Comparison of Results

The simulation results gave us a good idea about the conductivity of the carbon microfiber which matches the shielding effectiveness with the measured results. Previously  $S_{21}$  results were compared, and it was observed that the conductivity values from  $1000 S/m$  to  $4000 S/m$  were giving the close simulation values in comparison to the  $S_{21}$  measurements. Now we are comparing the analytical shielding effectiveness values of these conductivities with the simulated and measured results.

Figure 28 shows the comparison of the measured shielding effectiveness for the carbon microfiber sample 0323 with the simulated shielding effectiveness for the conductivity values of  $1000 S/m$ ,  $1500 S/m$ ,  $2000 S/m$  and  $4000 S/m$ , and the analytical shielding values for the same conductivities. The simulated shielding values for these conductivity values are within the  $8 - 10 dB$  of each other, and all of these simulated shielding effectiveness plots are from  $5 dB$  to  $13 dB$  from the measured results. The variation from the analytical values are from  $8 dB$  to  $15 dB$  where as it is highest for the lower end of the frequency range specifically from  $1 GHz$  to  $1.5 GHz$ .

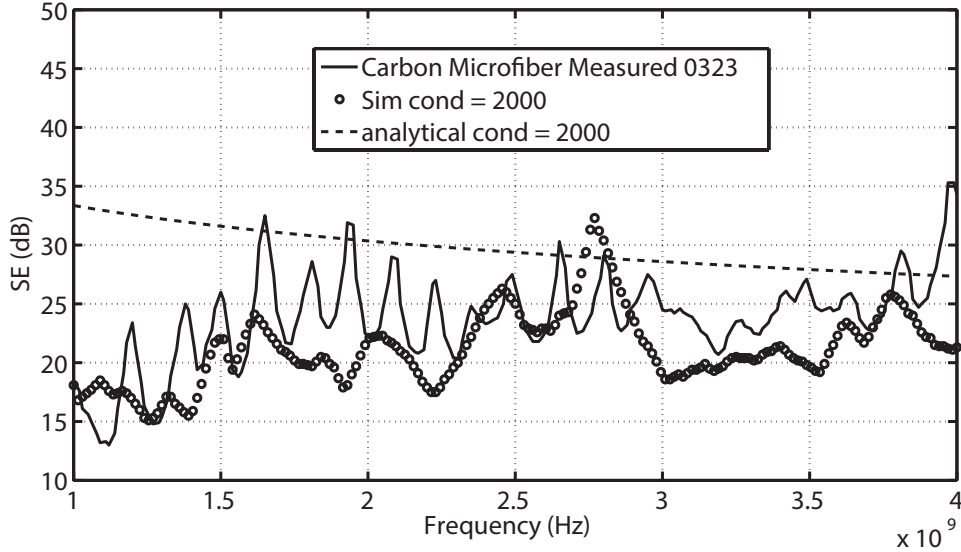


Figure 29. Shielding effectiveness comparison for conductivity  $2000 \text{ S/m}$ .

From this comparison we conclude that  $2000 \text{ S/m}$  can be the closest value of the conductivity for the carbon microfiber to assume where both the simulated and analytical shielding values are within  $5 \text{ dB}$  except for the range  $1 \text{ GHz}$  to  $1.5 \text{ GHz}$ . This is shown in Figure 29. The simulated values are varying only in the  $2 \text{ dB}$  to  $3 \text{ dB}$  range of the measured shielding effectiveness and the analytical values are in the  $5 \text{ dB}$  range from the measured shielding effectiveness results excluding the exception stated above.

The possibility for this variation of the result for the lower frequency range may depend on the ideal metallic sheet behavior that all of the signal is incident upon the sheet in comparison to the actual measurement setup where at the lower frequencies the wavelength increases and may come through the side of the sheet as the sheet size is infinite. Or the other case may be that the conductivity of the carbon microfiber is also dependent on the frequency while for the analytical calculation, it remains the same for the whole frequency range.

## 5.2. Conclusions

This research work focuses on the electromagnetic shielding properties of the carbon microfiber material. For this purpose, measurement of shielding effectiveness, simulation of the measurement environment in HFSS *v.15.0*, and analytical derivation have been investigated. The effect of carbon microfiber material on heating /cooling of a metallic enclosure has also been studied.

The results of the shielding effectiveness for carbon microfiber showed good agreement with the metallic shield thus making the carbon microfiber a suitable contender for the replacement of the metallic shield in EM shielding applications. A shielding effectiveness of about 25 *dB* for the proposed setup was observed for the aluminum sheet and the carbon microfiber shield. The simulation results and the measurements showed good agreement for this measurement setup. This setup hence verified the reliability of the simulations with the measurements. Moreover, the shielding effectiveness for the ideal carbon microfiber shield are computed analytically and are compared with the simulation and measurement results. It is observed that there is minor deviation (about 5 *dB*) in the analytical results because of the assumption of the ideal shield. As the actual setup included antennas, free space and finite sheet in the chamber.

Furthermore, heating up and cooling down time of a metallic chamber was observed, and it was noted that the metallic enclosure heated less with its one wall replaced with carbon microfiber. Also, the enclosure cooled down faster than the complete metallic enclosure. This heating/cooling property gives an added advantage in comparison to the metallic shields and enclosures. The results of the shielding effectiveness showed that the carbon microfiber is capable of blocking an EM wave over the range from 1 *GHz* to 4 *GHz*. These composite materials have a shielding property that is same as that of metals but are flexible and light weight as compared

to the metals. Carbon microfibers also have an anti-corrosion property. Thus, the carbon microfiber can be used in the medical appliances industry, electronic devices, and aircraft for the shielding of the EM waves as well as for the cooling/heating of the electronic equipment.

## BIBLIOGRAPHY

- [1] Yang S., Lozano K., Lomeli A., Foltz H. D., Jones R., “Electromagnetic interference shielding effectiveness of carbon nanofiber/LCP composites”, *Composites: Part A*, Vol. 36, pp. 691-697, 2005.
- [2] Chung D. D. L., “Electromagnetic interference shielding effectiveness of carbon materials”, *Elsevier Science Ltd., Carbon*, Vol. 39, pp. 279-285, 2001.
- [3] Xing L., Liu J., Ren S., “Study on electromagnetic property of short carbon fibers and its application to radar absorbing”, *Cailiao Gongcheng/J Mater Eng.*, pp. 1921, 1998.
- [4] Rupprecht L., Hawkinson C., “Conductive plastics for medical applications”. *Medical Device & Diagnostic Industry*, 1999.
- [5] Tan S., Zhang M., Zeng H., “Electroconductive polymer composite for shielding EMI”, *Cailiao Gongcheng/J Mater Eng.*, pp. 69, 1998.
- [6] Kolyer J. M., “Environmentally resistant, conductive adhesive bonds for radio frequency (RF) shielding”, *Proc. 43rd Int. SAMPE Symp. Exhib., Covina, California, USA*, vol. 43, pp. 810822, 1998.
- [7] Olivero D. A., Radford D. W., “Multiple percolation approach to EMI shielding composites incorporating conductive fillers”, *Reinforced Plastics & Composites*, pp. 674690, 1998.
- [8] Sau K. P., Chaki T. K., Chakraborty A., Khastgir D., “ Electromagnetic interference shielding by carbon black and carbon fibre filled rubber composites”, *Plastics Rubber & Composites Processing & Applications*, pp.291-297, 1997.



- [9] Miyashita K., Imai Y., “Study on shielding materials for electromagnetic waves”, *Int. Progr. Urethanes*, pp. 195-218, 1993.
- [10] Ma C. M., Hu A. T., Chen D.K. , “Processability, electrical and mechanical properties of EMI shielding ABS composites”, *Polymers & Polymer Composites*, pp. 93-99, 1993.
- [11] Li L., Chung D. D. L., “Electrical and mechanical properties of electrically conductive polyethersulfone composite”, *Composites*, pp. 215-224, 1994.
- [12] Li L., Chung D. D. L., “Effect of viscosity on the electrical properties of conducting thermoplastic composites made by compression molding of a powder mixture”, *Polym. Composites*, pp. 46772, 1993.
- [13] Kelly A., “Composites in context”, *Compos Sci Technology*, Vol. 23, Issue. 3, pp. 171-199, 1985.
- [14] Hull D., Clyne T. W., “An Introduction to Composite Materials”, Second edition, Cambridge University Press, 1996.
- [15] Pilato L. A., Michno M. J., “Advanced Composite Material”, Berlin: Springer-Verlag, 1994.
- [16] Gay D., Hoa S. V., Tsai S. W., “Composite materials: design and applications”, Boca Raton, FL: CRC Press, 2003.
- [17] Shui X., Chung D. D. L., “Nickel filament polymer matrix composites with low surface impedance and high electromagnetic interference shielding effectiveness”, *J Electron Mater*, pp. 928-934, 1997.

- [18] Luo X., Chung D. D. L., “Electromagnetic interference shielding reaching 130 dB using flexible graphite”, *Elsevier Science Ltd, Carbon 34*, vol. 10, pp. 1293-1294, 2001.
- [19] [online] [www.ansoft.com](http://www.ansoft.com)
- [20] Henry W. Ott, “Electromagnetic Compatibility Engineering“, John Wiley & sons, 2009.
- [21] Hayt, W. H. Jr. “Engineering Electromagnetics“, McGraw Hill, 8th. ed. New York, 2012
- [22] [online] [www.fibreglast.com](http://www.fibreglast.com)
- [23] [online] [www.jdr.sagepub.com](http://www.jdr.sagepub.com)
- [24] [online] [www.nanotechweb.org/cws/article/lab/58172](http://www.nanotechweb.org/cws/article/lab/58172)
- [25] [online] [www.spacedaily.com](http://www.spacedaily.com)